

Design, Synthesis, and Molecular Docking of Novel Benzothiazinone Derivatives as DprE1 Inhibitors with Potential Antitubercular Activities

M. S. Raghu^a, Amar Yasser Jassim^b, K. Yogesh Kumar^c, Fahd Alharethy^d,
M. K. Prashanth^{e,*}, and Byong-Hun Jeon^{f,**}

^a Department of Chemistry, New Horizon College of Engineering, Bengaluru 560103 India

^b Department of Marine Vertebrate, Marine Science Center, University of Basrah, Basrah, 61001 Iraq

^c Department of Chemistry, Faculty of Engineering and Technology, Jain University, Ramanagara, 562112 India

^d Department of Chemistry, College of Science, King Saud University, Riyadh, 11451 Saudi Arabia

^e Department of Chemistry, BNM Institute of Technology, Bengaluru, 560070 India

^f Department of Earth Resources and Environmental Engineering, Hanyang University, 222, Wangsimni-ro, Seongdong-gu, Seoul, 04763 Republic of Korea

*e-mail: prashanthmk87@gmail.com; **e-mail: bhjeon@hanyang.ac.kr

Received September 11, 2024; revised September 25, 2024; accepted October 1, 2024

Abstract—Objective: As a possible antitubercular agent, we disclose in this study the design and synthesis of a novel series of benzothiazinone derivatives (**Va–Vi**), contributing to the worldwide fight to eradicate TB, one of the deadliest infectious killers in the world. **Methods:** The newly synthesized benzothiazinone derivatives were characterized using various spectroscopic and elemental analysis techniques. The antituberculosis activity of the synthesized benzothiazinone derivatives was evaluated against drug-sensitive *Mtb* H37Rv and MDR-TB strains. To explain their inhibitory qualities, potent compounds underwent molecular docking studies. The synthetic molecules' ability to function as lead-like molecules and the drug-likeness of the compounds were computed using the SwissADME online tool. **Results and Discussion:** With a MIC of 0.01 and 0.21 μM , respectively, compound (**Vi**) showed the most promising antitubercular efficacy against drug-sensitive *Mtb* H37Rv and MDR-TB strains. Four of the nine studied compounds had strong DprE1 inhibitory action, with IC_{50} values ranging from 0.02 to 0.79 μM . The molecular docking findings indicated that these compounds had a high docking score and a strong binding affinity to the target DprE1 protein's active pocket. **Conclusions:** The current study demonstrated the potential significance of novel benzothiazinone derivatives as antitubercular prospects, and further investigation into optimization may lead to the creation of new antitubercular medication candidates.

Keywords: benzothiazinone, tuberculosis, DprE1, molecular docking, drug-likeness

DOI: 10.1134/S1068162025010042

INTRODUCTION

Tuberculosis (TB) is one of the most devastating infectious diseases in the world. It is also one of the most contagious diseases. Despite being a disease that dates back thousands of years, significant money and effort are still dedicated to making tuberculosis a thing of the past [1]. About 25% of the global population is thought to be infected with the TB bacteria [2]. An estimated 7.5 million cases of TB were recorded worldwide in 2022, with 1.3 million cases of the disease being fatal [3].

Furthermore, surveillance data highlight the persistent issue of multidrug-resistant tuberculosis (MDR-TB), which can be attributed to noncompliance with treatment regimens or comorbidities that impede immune response [4]. The necessity to find innovative medications to combat tuberculosis and the emergence of drug resistance have prompted ongoing attempts to improve the efficacy of the arduous and protracted therapy. Therefore, the aforementioned facts underscore the need to design new agents that surpass existing ones by increasing their effectiveness and overcoming acquired resistance.

Over the past few decades, numerous evaluations and surveys have been conducted on the various scaffolds utilized in the search for antitubercular drugs, as well as antitubercular agents and targets [5]. Among the many TB targets that have been explored, DprE1 stands out as one of the most promising for developing novel antituberculosis drugs. It has been found that DprE1 is essential for the survival of *Mtb*, including MDR strains [6]. DprE1, a flavoenzyme, is crucial for the construction of the cell walls of mycobacteria. The synthesis of arabinogalactan and lipoarabinomannan is initiated by the epimerization of decaprenyl-phospho-ribose (DPR) to decaprenyl-phospho-arabinose (DPA), which is catalyzed by DprE1 and DprE2 [7, 8]. The initial phase of the epimerization process is initiated by DprE1, which oxidizes DPR to decaprenylphosphoryl-2-ketoribose (DPX), an intermediate. Afterwards, DPX is converted into DPA by the NADH-dependent enzyme DprE2 [9]. DprE1 is a target vulnerable to epimerization that occurs in the periplasmic space [10], making it an attractive target for the development of new treatment options for TB.

The pharmaceutical industry has extensively utilized the bioactivity potential of heterocyclic compounds to find novel treatment options. A wide variety of pharmacological actions are exhibited by several groups of heterocyclic compounds [11]. One family of heterocyclic compounds containing sulfur that is significant in drug development is benzothiazinones. They exhibit a range of biological properties, including antibacterial, antifungal, antituberculosis, anticancer, and anti-inflammatory effects [12].

Benzothiazinones represent an intriguing class of novel anti-TB medication options. By interfering with the production of arabinan, 8-nitrobenzothiazinones have proven to be a highly effective family of antimycobacterial agents, inhibiting the growth of *Mtb* even at nanomolar concentrations [13]. BTZs have recently attracted considerable attention as the most sophisticated scaffold for targeting DprE1, and several series of BTZ derivatives have been published [14–16]. The preclinical candidate PBTZ169, which emerged from lead modifications of BTZ043, has shown significant potential in treating TB and is about to enter clinical trials (Fig. 1) [13]. Therefore,

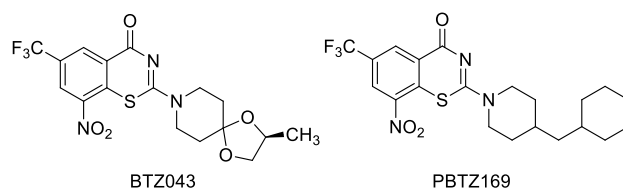


Fig. 1. Reported BTZ type DprE1 inhibitors in phase II clinical trials.

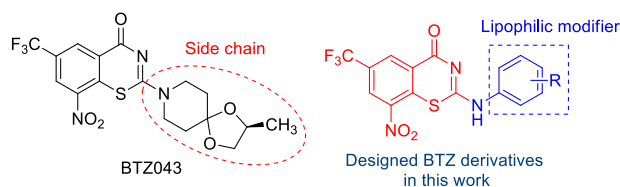


Fig. 2. Design rationale for DprE1 inhibitors.

benzothiazinones have demonstrated encouraging anti-tubercular activity and provide strong support for the development of DprE1 inhibitors for the treatment of tuberculosis [17].

Despite progressing to clinical trials, both benzothiazinones exhibited unsatisfactory drug-like characteristics. Due to its high plasma protein binding fraction, the more potent second-generation PBTZ169 is held responsible for its poor *in vivo* bioavailability [18]. Nevertheless, the subpar physicochemical and pharmacokinetic properties of these compounds drove us to create new ones. Furthermore, SAR studies and thorough mechanistic investigations indicated that the nitro group at position 8 and the sulfur atom at position 1 are crucial for activity, while the trifluoromethyl group at position 6 is also essential for preserving BTZ's anti-tubercular action [19]. Considering the aforementioned information and adhering to our research endeavors that focus on the design and synthesis of new medicinal agents [20–32], this study aims to design and synthesize a new range of benzothiazinone derivatives that possess exceptional drug-like characteristics and prove to be highly effective and selective anti-TB agents. To increase the diversity of BTZ compounds, we demonstrate the modification of the side chain of the BTZ molecule through the inclusion of a substituted phenyl ring as a lipophilic modifier (Fig. 2).

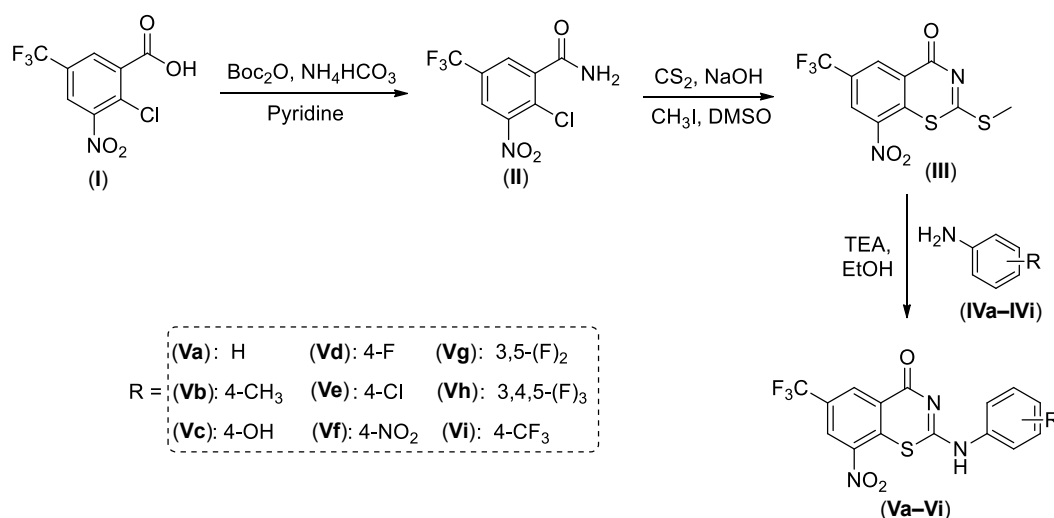
Moreover, their interactions with the target DprE1 protein were determined using molecular docking studies

RESULTS AND DISCUSSION

Chemical Synthesis

Medicinal chemistry relies significantly on benzothiazinones as scaffolds, and the literature has documented enormous efforts made to synthesize these compounds. Therefore, benzothiazinone derivatives were produced in the current investigation. Scheme 1 shows the synthetic pathway for the target compounds (**Va–Vi**). Using di-*tert*-butyl dicarbonate and ammonium bicarbonate, the synthesis began by forming 2-chloro-3-nitro-5-(trifluoromethyl)benzamide (**II**) from 2-chloro-3-nitro-5-(trifluoromethyl)benzoic acid (**I**) under moderate conditions [33]. Mass spectroscopy and ¹H and ¹³C NMR spectra provided excellent structural characterizations for all of the newly synthesized compounds. The amide proton and the –CH protons of the phenyl ring are represented by three singlet peaks in the ¹H NMR spectrum of compound (**II**), which are located at 7.83, 8.46, and 8.70 ppm, respectively. Furthermore, the structure of compound (**II**) was confirmed by analytical and mass spectral data. Additionally, the reaction of compound (**II**) with methyl iodide and carbon disulfide produced the key intermediate

2-(methylthio)-8-nitro-6-(trifluoromethyl)-4*H*-benzo[*e*]-[1,3]thiazin-4-one (**III**). The synthesis of compound (**III**) was confirmed by the appearance of a new methyl group peak at 2.72 ppm and the disappearance of the amide singlet peak at 7.83 ppm in the ¹H NMR spectrum of compound (**III**). Ultimately, the key intermediate **3** was treated with various substituted amines (**VIa–VIi**) in the presence of triethylamine in EtOH, resulting in a good yield of 86–93% of the target products, (**Va–Vi**). The emergence of a –NH peak between 4.13 and 4.29 ppm and the elimination of the singlet peak at 2.72 ppm in the ¹H NMR spectra of compounds (**Va–Vi**) confirmed the synthesis of the benzothiazinone derivatives (**Va–Vi**). The aromatic protons of compounds (**Va–Vi**) resonated within their usual range, according to the ¹H NMR spectra. Compound (**Vb**) exhibited a singlet peak at 2.12 ppm, indicating the presence of a methyl group on the phenyl ring, whereas compound (**Vc**) had a singlet peak at 5.70 ppm, signifying the presence of a hydroxyl group. All of the compounds' mass spectra revealed molecular ion peaks that matched the molecular weights of compounds (**Va–Vi**). Moreover, there was a noteworthy degree of concurrence between the elemental analysis results and the values obtained from theoretical computations and experimental measurements.



Scheme 1. The synthetic pathway of the target compounds (**Va–Vi**).

Antitubercular Activity

All of the target compounds (**Va–Vi**) were evaluated for their *in vitro* antitubercular activity against drug-sensitive *Mtb* H37Rv and MDR-TB strains once the synthesis was completed. Table 1 presents the findings of the anti-TB investigations. The ability of PBTZ169 to inhibit drug-sensitive *Mtb* H37Rv and MDR-TB strains was used as a control. With MIC values ranging from 0.01 to 9.82 and 0.21 to 18.81 μM , respectively, all of the newly synthesized compounds demonstrated moderate to significant inhibition against both the drug-sensitive *Mtb* H37Rv and MDR-TB strains, according to the obtained data. Among the newly synthesized compounds, 8-nitro-6-(trifluoromethyl)-2-((4-(trifluoromethyl)phenyl)amino)-4*H*-benzo[*e*][1,3]thiazin-4-one (**Vi**) had the highest potency, exhibiting inhibition against both drug-sensitive *Mtb* H37Rv and MDR-TB strains with MIC values of 0.01 and 0.21 μM , respectively. This was more potent than the corresponding compounds (**Va–Vh**) and the reference drug PBTZ169. With MIC values of 0.05 and 0.41 μM , respectively, compound (**Vf**) was the second most potent in this series against both drug-sensitive *Mtb* H37Rv and MDR-TB strains. Compounds (**Va–Ve**) showed less inhibitory effect against drug-sensitive *Mtb* H37Rv and MDR-TB strains, whereas compounds (**Vg**) and (**Vh**) demonstrated moderate inhibitory activity. These findings unequivocally indicate

Table 1. The anti-TB activity of the compounds (**Va–Vi**)

Compound	MIC (μM)	
	<i>Mtb</i> H37Rv	MDR <i>Mtb</i>
(Va)	5.26 \pm 0.72	8.18 \pm 0.94
(Vb)	8.25 \pm 0.64	12.92 \pm 1.03
(Vc)	9.82 \pm 0.97	15.81 \pm 1.26
(Vd)	2.64 \pm 0.32	4.83 \pm 0.42
(Ve)	3.19 \pm 0.81	5.04 \pm 0.95
(Vf)	0.05 \pm 0.01	0.41 \pm 0.07
(Vg)	0.63 \pm 0.26	1.05 \pm 0.42
(Vh)	0.48 \pm 0.18	1.59 \pm 0.33
(Vi)	0.01 \pm 0.003	0.21 \pm 0.09
PBTZ169	0.01 \pm 0.001	0.25 \pm 0.06

that, compared to the other compounds, (**Vf**) and (**Vi**) exhibited significantly greater antitubercular activity.

Cytotoxicity

Using the MTT method, the *in vitro* cytotoxicity of the newly synthesized compounds (**Va–Vi**) was evaluated against the normal WI-38 cell line. Table 2 displays the observed CC_{50} values for these compounds. Table 2 indicates that, even at a maximum dosage of 64 μM , none of the tested compounds exhibited lethal effects on the WI-38 cell line, indicating that these compounds have a significant amount of potential for use as antitubercular drugs. With respect to *Mtb* H37Rv, the potent compounds (**Vf**) and (**Vi**) had SI values of 1280 and 6400, while for MDR *Mtb*, they were 156.10 and 304.76, respectively. Against *Mtb* H37Rv and MDR *Mtb*, PBTZ169 demonstrated an SI of 6400 and 256, respectively.

DprE1 Inhibition Studies

The newly synthesized compounds were assessed for their ability to inhibit DprE1. The FPR substrate was used for the DprE1 activity test. Table 3 presents the findings. The strong antitubercular properties of the synthesized compounds and their DprE1 inhibitory activities were shown to be correlated, according to the findings. The synthesized compounds exhibit IC_{50} values between 0.12 and 6.81 μM , indicating that they inhibit DprE1. Four of the nine compounds studied showed strong inhibitory

Table 2. *In vitro* cytotoxic activity against WI-38 cell line and selectivity index for the target compounds (**Va–Vi**)

Compound	CC_{50} (μM)	Selectivity index (SI)	
	WI-38	<i>Mtb</i> H37Rv	MDR <i>Mtb</i>
(Va)	>64	12.17	7.82
(Vb)	>64	7.76	4.95
(Vc)	>64	6.51	4.05
(Vd)	>64	24.24	13.25
(Ve)	>64	20.06	12.70
(Vf)	>64	1280	156.10
(Vg)	>64	101.59	60.95
(Vh)	>64	133.33	40.25
(Vi)	>64	6400	304.76
PBTZ169	>64	6400	256

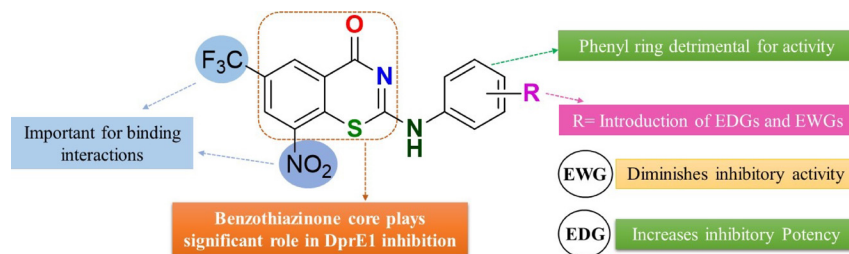


Fig. 3. SAR summary of the synthesized compounds against DprE1 inhibition.

action against DprE1, with IC_{50} values ranging from 0.02 to 0.79 μM . The IC_{50} values of compounds (**Vf**) and (**Vi**) were 0.07 and 0.02 μM , respectively, while compounds (**Vg**) and (**Vh**) showed varying IC_{50} values of 0.79 and 0.56 μM , respectively. The reference drug PBTZ169 was found to have an IC_{50} of 0.02 μM .

Relying on the DprE1 inhibitory activities shown in Table 3, the structure-activity relationship (SAR) of the newly synthesized benzothiazinones (**Va–Vi**) may be determined. The relationship between structure and activity can be found through the SAR analysis of benzothiazinones, which also provides suggestions for structural changes that may enhance activity. Understanding the mechanisms behind DprE1 inhibitory action for benzothiazinones is facilitated by SAR analysis. In-depth SAR investigations were carried out, with particular attention to the central core of the benzothiazinone scaffold and its various substitution patterns. In this section, we examined the effects of substituents known as electron-donating groups (EDGs) and electron-

withdrawing groups (EWGs) on the phenyl ring linked to the benzothiazinone core by an $-\text{NH}$ linker concerning the SAR. These results imply that the observed variations in the DprE1 inhibitory activities were caused by different substituents. Only a limited number of substitution patterns on the phenyl ring connected to the benzothiazinone core had an impact on these inhibitory activities. The nature of the substituents had a significant impact on the disparity in their potential (Fig. 3).

Based on the results obtained, compounds (**Ve–Vi**) demonstrate an increase in DprE1 inhibitory activity when EWG groups are present on the phenyl ring connected to the benzothiazinone core, but compounds (**Vb**) and (**Vc**) bearing EDG demonstrate a decrease in inhibitory activity. The compounds (**Ve–Vi**) possess EWGs; however, compound (**Vi**) exhibits higher activity compared to compounds (**Ve–Vh**). This suggests that compound (**Vi**)'s electron-withdrawing trifluoromethyl group is more efficient in enhancing DprE1 inhibitory action than the other EWGs in this series. Through bonding interactions, trifluoromethyl groups have a great affinity for the active site of enzymes. Furthermore, because of their greater lipophilicity than other EWGs, trifluoromethyl substituents are advantageous. Furthermore, the trifluoromethyl group enhances the acidity of the aromatic ring and modifies its electrostatic interactions with the substrate by decreasing its electrical density. Compound (**Vf**), which has a nitro group substituted on its phenyl ring, was shown to have greater inhibitory action than compounds (**Vd**), (**Ve**), (**Vg**), and (**Vh**), which had fluoro, chloro, 3,5-difluoro, and 3,4,5-trifluoro groups, respectively. Additionally, compound (**Vh**) surpassed compound (**Vg**) in terms of potency, mainly because it has

Table 3. Inhibition of DprE1 by target compounds (**Va–Vi**)

Compound	IC_{50} (μM)
(Va)	3.89 ± 0.94
(Vb)	5.40 ± 1.03
(Vc)	6.81 ± 1.15
(Vd)	1.93 ± 0.62
(Ve)	3.26 ± 0.97
(Vf)	0.07 ± 0.02
(Vg)	0.79 ± 0.33
(Vh)	0.56 ± 0.18
(Vi)	0.02 ± 0.004
PBTZ169	0.02 ± 0.007

a 3,4,5-trifluoro substituent, which increases the scaffold's inhibitory potential in comparison to compound (Vg), which contains a 3,5-difluoro substituent. Conversely, compounds (Vb) and (Vc) with electron-donating methyl and hydroxy groups on the phenyl ring, respectively, greatly diminish the inhibitory effect when compared to compounds containing EWGs (Vd–Vi) and an unsubstituted phenyl ring (Va). The entire work suggests that the phenyl ring attached to benzothiazinone core molecules with EWGs is essential for the inhibition of DprE1.

Molecular Docking

To provide concise details for additional structural optimization, the binding mechanism of the compounds was clarified using molecular docking. This study utilized molecular docking to examine potential binding mechanisms. A crucial step in the synthesis of lipoarabinomannan and arabinogalactan, two substances required for cell wall biosynthesis, is catalyzed by DprE1, a vital flavoenzyme in *Mtb* [34]. In light of this, DprE1 represents an *Mtb* target that may be used to develop new potent drugs [35]. Consequently, the DprE1 protein (PDB ID: 4P8L) was selected as a potential molecular docking target. The most effective compounds (Vf–Vi) in this series were chosen for the molecular docking analysis based on *in vitro* studies and DprE1 inhibitory activity. Potent compounds were docked with target proteins using AutoDock Vina, which was implemented in UCSF Chimera. The 2D and 3D docked interactions of these potent compounds with the target 4P8L protein are displayed in Figs. 4 and 5, respectively. Table 4 summarizes the quantitative metrics for these compounds, including the residue interactions, bond distances, and docking scores. Based on the docking data, it was shown that all the potent compounds had good docking scores in the 4P8L protein's active pocket. This is because the compounds attach to the amino acid residues of the active site *via* H-bonds and other interactions that strengthen the binding. The target 4P8L protein binding site exhibited a comparable binding pattern for compounds (Vf–Vi) when compared to the reference ligand PBTZ169, which had a docking

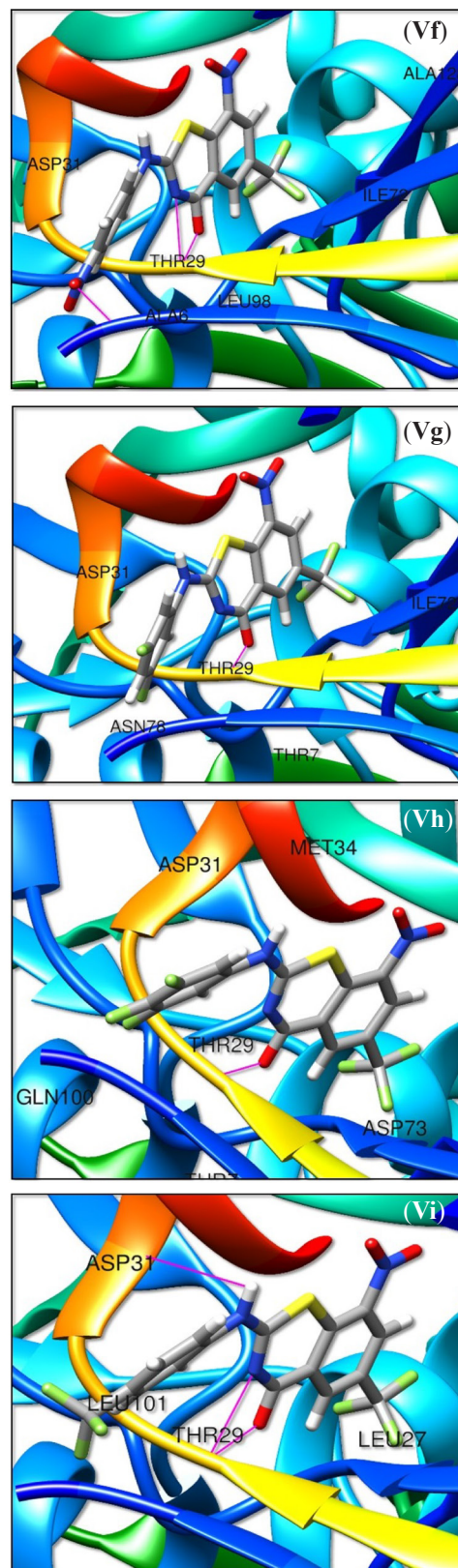


Fig. 4. Docking interactions of potent compounds with target 4P8L protein.

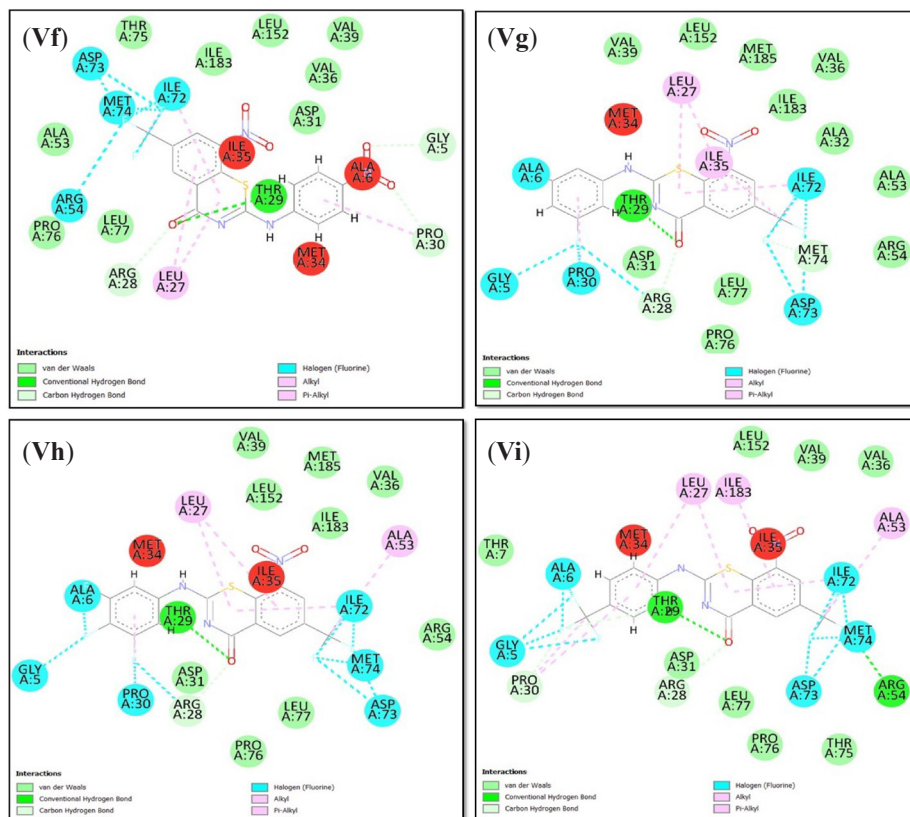


Fig. 5. 2D interactions of potent compounds with target 4P8L protein.

score of -9.47 kcal/mol. The estimated docking scores of these compounds were -9.43 , -8.46 , -8.95 , and -9.68 kcal/mol, respectively. The most effective molecule in the series, compound (Vi), ranked first in the protein-ligand interaction profile against the 4P8L protein, showing an H-bond with Asp-31 and Thr-29, with bond distances of 1.45 and 1.21 Å, respectively. Furthermore, this molecule established a π -alkyl connection between the compound's phenyl and benzothiazinone rings and residues Leu-27, Ala-53, and Ile-183. Compound (Vf) established a π -alkyl contact with the target protein's Leu-27 residue and had H-bonding interactions with the Ala-6 and Thr-29 residues, with bond distances of 0.57 and 1.12 Å, respectively. Compounds (Vg) and (Vh) were found to interact with the Thr-29 residue through a hydrogen bond, with bond distances of 0.95 and 1.18 Å, respectively, upon docking with the target protein. Additionally, compounds (Vg) and (Vh) created π -alkyl interactions with the target protein's Leu-27 and Ile-35

residues and Ala-53 and Leu-27 residues, respectively. The results of the docking study confirmed the main idea of this work and demonstrated the compounds' potent inhibitory effects. Lastly, the experimental results from the antitubercular investigation and the docking analysis show a consistent correlation.

Drug-Likeness Prediction

A key criterion for determining if a molecule has the potential to be a drug is its drug-likeness. The Lipinski Rules of Five were used to identify the chemical descriptors and drug-likeness characteristics of the compounds using the SwissADME program [36]. When designing and developing new drugs, pharmaceutical chemists use Lipinski's Rule of Five to forecast the oral bioavailability of potential leads or therapeutic molecules. A molecule would not be considered orally active by Lipinski's Rule of Five if 2 or more of the 5 requirements were not met. The drug-like characteristics

Table 4. Binding interactions of potent compounds with target protein

Compound	Docking score (kcal/mol)	Interacting residues			
		H-bond	bond length (Å)	hydrophobic	π -alkyl
(Vf)	-9.43	Ala-6 Thr-29	0.57 1.12	Gly-5, Arg-28, Pro-30, Asp-31, Val-36, Val-39, Ala-53, Arg-54, Ile-72, Asp-73, Met-74, Thr-75, Pro-76, Leu-77, Leu-152, Ile-183	Leu-27
(Vg)	-8.46	Thr-29	0.95	Gly-5, Ala-6, Arg-28, Asp-31, Ala-32, Val-36, Val-39, Ala-53, Arg-54, Ile-72, Asp-73, Met-74, Pro-76, Leu-77, Leu-152, Ile-183, Met-185	Leu-27, Ile-35
(Vh)	-8.95	Thr-29	1.18	Gly-5, Ala-6, Arg-28, Pro-30, Asp-31, Val-36, Val-39, Arg-54, Ile-72, Asp-73, Met-74, Pro-76, Leu-77, Leu-152, Ile-183, Met-185	Leu-27, Ala-53
(Vi)	-9.68	Thr-29 Asp-31	1.45 1.21	Gly-5, Ala-6, Arg-28, Pro-30, Val-36, Val-39, Arg-54, Ile-72, Asp-73, Met-74, Thr-75, Pro-76, Leu-77, Leu-152	Leu-27, Ala-53, Ile-183
PBTZ169	-9.47	Thr-29	1.49	Gly-5, Thr-7, Arg-28, Pro-30, Asp-31, Met-34, Val-36, Val-39, Ile-52, Ala-53, Arg-54, Ile-72, Met-74, Pro-76, Leu-152	Leu-27, Leu-77, Ile-183

Table 5. Predicted physicochemical parameters of the titled compounds

Compound	MW	Rotatable bonds	HBA	HBD	log <i>P</i>	Molar refractivity	log <i>K_p</i> (cm/s)	TPSA (Å ²)
(Va)	367.30	4	7	1	1.91	89.26	-5.76	116.05
(Vb)	381.33	4	7	1	2.13	94.22	-5.59	116.05
(Vc)	383.30	4	8	2	1.46	91.28	-6.12	127.28
(Vd)	385.29	4	8	1	2.01	89.22	-5.80	116.05
(Ve)	401.75	4	7	1	2.18	94.27	-5.53	116.05
(Vf)	412.30	5	9	1	1.56	98.08	-6.16	134.87
(Vg)	403.28	4	9	1	2.03	89.17	-5.84	116.05
(Vh)	421.27	4	10	1	1.95	89.13	-5.88	116.05
(Vi)	435.30	5	10	1	1.96	94.26	-5.55	116.05

of the newly synthesized compounds (Va–Vi) are displayed in Table 5. Since every metric complies with Lipinski's Rule of Five, it was expected that all of the newly synthesized compounds, (Va–Vi), would have adequate oral bioavailability. Remarkably, the newly synthesized molecules have a molecular weight (< 500) in the range of 367.30 to 435.30. It was determined that the investigated compounds contained 1–2 and 7–10 HBD, respectively. Lipophilicity (log*P* value) and TPSA values are two important metrics for determining oral bioavailability for pharmacological substances [37]. A possible drug-like candidate's log*P* value should, in

general, fall between 0 and 5. The greater the lipophilicity of the compound, the higher the log*P* value. The log*P* values of all the compounds under investigation ranged from 1.46 to 2.18. It is anticipated that molecules having TPSA values of 140 Å² or above will have inadequate intestinal absorption. Nine molecules examined in this study have TPSA findings that fall within this range (< 140 Å²). Additionally, the skin permeability log*K_p* falls between the typical range of -8.0 and -1.0. As a result, the data suggested that all the investigated molecules met Lipinski's criteria, suggesting that they all had characteristics similar to those of drugs.

EXPERIMENTAL

Materials. All the chemicals that were purchased commercially were utilized without further purification. The chemical shift values were expressed in parts per million (ppm), and the ^1H (400 MHz) and ^{13}C (100 MHz) NMR spectra were obtained using a Bruker AM 400 spectrometer with DMSO- d_6 solvent and TMS as the internal reference standard. A Perkin Elmer PE Sciex API/65 LC-MS apparatus was used to obtain the mass spectra of the molecules. A Perkin-Elmer 2400 Series II Elemental CHN analyzer was used to perform the elemental analysis.

Synthesis of 2-chloro-3-nitro-5-(trifluoromethyl)benzamide (II). At room temperature, a stirred solution of compound (I) (10 mmol), pyridine (6.5 mmol), and di-*tert*-butyl dicarbonate (13 mmol) in 1,4-dioxane was added to ammonium bicarbonate (13 mmol). The reaction was stirred for 8 h at room temperature. After the completion of the reaction, the mixture was diluted with water and extracted with ethyl acetate. The organic layer was washed with water, dried over anhydrous sodium sulfate, and the solvent was evaporated to obtain compound (II) as a white solid. Yield: 86%. mp: 112–114°C. ^1H NMR (400 MHz, DMSO- d_6), ppm: 7.83 (s, 2H, $-\text{NH}_2$), 8.46 (s, 1H, Ar-H), 8.70 (s, 1H, Ar-H). ^{13}C NMR (100 MHz, DMSO- d_6) δ : 122.4, 122.7, 130.1, 131.0, 131.3, 133.5, 148.1, 168.2. MS: m/z 268 [$M + 1$]. Anal. Calcd. for $\text{C}_8\text{H}_4\text{ClF}_3\text{N}_2\text{O}_3$: C, 35.78; H, 1.50; N, 10.43. Found: C, 35.75; H, 1.46; N, 10.48.

Synthesis of 2-(methylthio)-8-nitro-6-(trifluoromethyl)-4H-benzo[e][1,3]thiazin-4-one (III). Compound (II) (5 mmol) was gradually added to the mixture of NaOH (1.5 eq), DMSO (10 mL), and carbon disulfide (10 mmol) after it had been cooled between 10 and 15°C. After adding 5 mmol of methyl iodide to the resultant liquid, the reaction was stirred for 30 min. After the reaction was completed, ethyl acetate was used to extract the product from the reaction mixture and dilute it with water. To obtain compound (III), a yellow solid, the organic layer was washed with water, dried over anhydrous sodium sulfate, and the solvent was removed. Yield: 91%. mp.: 133–135°C. ^1H NMR

(400 MHz, DMSO- d_6), ppm: 2.72 (s, 3H, $-\text{CH}_3$), 8.21 (s, 1H, Ar-H), 8.68 (s, 1H, Ar-H). ^{13}C NMR (100 MHz, DMSO- d_6), ppm: 14.3, 122.7, 127.6, 129.2, 132.1, 132.5, 138.4, 147.8, 162.8, 167.7. MS: m/z 323 [$M + 1$]. Anal. Calcd. for $\text{C}_{10}\text{H}_5\text{F}_3\text{N}_2\text{O}_3\text{S}_2$: C, 37.27; H, 1.56; N, 8.69. Found: C, 37.25; H, 1.53; N, 8.74.

General procedure for the synthesis of compounds (Va–Vi). To a mixture of compound (III) (5 mmol) in ethanol (10 mL) and triethylamine (5.2 mmol), different substituted anilines (IVa–IVi) (5 mmol) were gently added and heated at 60°C for 6 h. After the reaction, the mixture was cooled to room temperature, diluted with water, and extracted with ethyl acetate. The organic layer was washed with water and dried over anhydrous sodium sulfate. The organic phase was evaporated at reduced pressure, and the resultant substance was recrystallized with ethanol, yielding 85–93% of the target compounds (Va–Vi).

8-Nitro-2-(phenylamino)-6-(trifluoromethyl)-4H-benzo[e][1,3]thiazin-4-one (Va) [38]. Yield: 88%. mp: 167–169°C. ^1H NMR (400 MHz, DMSO- d_6), ppm: 4.15 (s, 1H, $-\text{NH}$), 7.21–7.30 (m, 5H, Ar-H), 8.25 (s, 1H, Ar-H), 8.64 (s, 1H, Ar-H). ^{13}C NMR (100 MHz, DMSO- d_6), ppm: 120.9, 122.1, 122.7, 127.6, 129.2, 129.6, 132.1, 132.6, 138.5, 139.4, 147.8, 159.3, 167.7. MS: m/z 368 [$M + 1$]. Anal. Calcd. for $\text{C}_{15}\text{H}_8\text{F}_3\text{N}_3\text{O}_3\text{S}$: C, 49.05; H, 2.20; N, 11.44. Found: C, 49.02; H, 2.16; N, 11.49.

8-Nitro-2-(*p*-tolylamino)-6-(trifluoromethyl)-4H-benzo[e][1,3]thiazin-4-one (Vb). Yield: 91%. mp: 175–177°C. ^1H NMR (400 MHz, DMSO- d_6), ppm: 2.12 (s, 3H, $-\text{CH}_3$), 4.27 (s, 1H, $-\text{NH}$), 7.56 (d, 2H, $J = 8.4$ Hz, Ar-H), 7.75 (d, 2H, $J = 8.4$ Hz, Ar-H), 8.23 (s, 1H, Ar-H), 8.65 (s, 1H, Ar-H). ^{13}C NMR (100 MHz, DMSO- d_6), ppm: 21.5, 116.2, 122.5, 127.6, 129.1, 129.8, 131.4, 132.4, 132.6, 136.4, 138.5, 147.9, 159.3, 167.7. MS: m/z 382 [$M + 1$]. Anal. Calcd. for $\text{C}_{16}\text{H}_{10}\text{F}_3\text{N}_3\text{O}_3\text{S}$: C, 50.40; H, 2.64; N, 11.02. Found: C, 50.37; H, 2.61; N, 11.08.

2-((4-Hydroxyphenyl)amino)-8-nitro-6-(trifluoromethyl)-4H-benzo[e][1,3]thiazin-4-one (Vc). Yield: 86%. mp: 172–174°C. ^1H NMR (400 MHz, DMSO- d_6), ppm: 4.13 (s, 1H, $-\text{NH}$), 5.70 (s, 1H, $-\text{OH}$), 6.78 (d, 2H,

$J = 7.6$ Hz, Ar–H), 6.88 (d, 2H, $J = 8.0$ Hz, Ar–H), 8.22 (s, 1H, Ar–H), 8.63 (s, 1H, Ar–H). ^{13}C NMR (100 MHz, DMSO- d_6), ppm: 116.4, 117.6, 122.7, 127.6, 129.2, 129.8, 132.3, 132.6, 138.5, 147.5, 148.9, 159.3, 167.5. MS: m/z 384 [$M + 1$]. Anal. Calcd. for $\text{C}_{15}\text{H}_8\text{F}_3\text{N}_3\text{O}_4\text{S}$: C, 47.00; H, 2.10; N, 10.96. Found: C, 46.95; H, 2.07; N, 11.02.

2-((4-Fluorophenyl)amino)-8-nitro-6-(trifluoromethyl)-4H-benzo[e][1,3]thiazin-4-one (Vd). Yield: 89%. mp: 153–155°C. ^1H NMR (400 MHz, DMSO- d_6), ppm: 4.28 (s, 1H, –NH), 7.59 (d, 2H, $J = 8.0$ Hz, Ar–H), 7.83 (d, 2H, $J = 8.4$ Hz, Ar–H), 8.23 (s, 1H, Ar–H), 8.64 (s, 1H, Ar–H). ^{13}C NMR (100 MHz, DMSO- d_6), ppm: 116.3, 120.8, 122.4, 127.3, 129.2, 132.1, 132.5, 135.2, 138.5, 147.8, 157.2, 159.2, 167.6. MS: m/z 386 [$M + 1$]. Anal. Calcd. for $\text{C}_{15}\text{H}_7\text{F}_4\text{N}_3\text{O}_3\text{S}$: C, 46.76; H, 1.83; N, 10.91. Found: C, 46.74; H, 1.80; N, 10.95.

2-((4-Chlorophenyl)amino)-8-nitro-6-(trifluoromethyl)-4H-benzo[e][1,3]thiazin-4-one (Ve). Yield: 91%. mp: 162–164°C. ^1H NMR (400 MHz, DMSO- d_6), ppm: 4.25 (s, 1H, –NH), 7.21 (d, 2H, $J = 8.8$ Hz, Ar–H), 7.82 (d, 2H, $J = 8.8$ Hz, Ar–H), 8.26 (s, 1H, Ar–H), 8.67 (s, 1H, Ar–H). ^{13}C NMR (100 MHz, DMSO- d_6), ppm: 120.8, 122.5, 127.4, 127.9, 129.2, 129.6, 132.3, 132.6, 137.5, 138.6, 147.8, 159.5, 167.5. MS: m/z 402 [$M + 1$]. Anal. Calcd. for $\text{C}_{15}\text{H}_7\text{ClF}_3\text{N}_3\text{O}_3\text{S}$: C, 44.84; H, 1.76; N, 10.46. Found: C, 44.81; H, 1.72; N, 10.51.

8-Nitro-2-((4-nitrophenyl)amino)-6-(trifluoromethyl)-4H-benzo[e][1,3]thiazin-4-one (Vf). Yield: 93%. mp: 182–184°C. ^1H NMR (400 MHz, DMSO- d_6), ppm: 4.26 (s, 1H, –NH), 6.98 (d, 2H, $J = 8.8$ Hz, Ar–H), 7.82 (d, 2H, $J = 7.6$ Hz, Ar–H), 8.26 (s, 1H, Ar–H), 8.67 (s, 1H, Ar–H). ^{13}C NMR (100 MHz, DMSO- d_6), ppm: 114.3, 122.7, 124.7, 127.6, 129.2, 132.1, 132.6, 137.9, 138.5, 145.6, 147.8, 159.3, 167.5. MS: m/z 413 [$M + 1$]. Anal. Calcd. for $\text{C}_{15}\text{H}_7\text{F}_3\text{N}_4\text{O}_5\text{S}$: C, 43.70; H, 1.71; N, 13.59. Found: C, 43.66; H, 1.69; N, 13.65.

2-((3,5-Difluorophenyl)amino)-8-nitro-6-(trifluoromethyl)-4H-benzo[e][1,3]thiazin-4-one (Vg). Yield: 86%. mp: 156–158°C. ^1H NMR (400 MHz, DMSO- d_6), ppm: 4.29 (s, 1H, –NH), 6.57 (s, 1H, Ar–H), 7.12 (s, 2H, Ar–H), 8.26 (s, 1H, Ar–H), 8.65 (s, 1H, Ar–H). ^{13}C NMR (100 MHz, DMSO- d_6), ppm: 94.7, 106.4, 122.7,

127.6, 129.2, 132.1, 132.6, 138.5, 147.2, 147.8, 158.5, 159.3, 167.7. MS: m/z 404 [$M + 1$]. Anal. Calcd. for $\text{C}_{15}\text{H}_6\text{F}_5\text{N}_3\text{O}_3\text{S}$: C, 44.67; H, 1.50; N, 10.42. Found: C, 44.64; H, 1.46; N, 10.47.

8-Nitro-6-(trifluoromethyl)-2-((3,4,5-trifluorophenyl)amino)-4H-benzo[e][1,3]thiazin-4-one (Vh). Yield: 88%. mp: 164–166°C. ^1H NMR (400 MHz, DMSO- d_6), ppm: 4.29 (s, 1H, –NH), 6.34 (s, 2H, Ar–H), 8.23 (s, 1H, Ar–H), 8.62 (s, 1H, Ar–H). ^{13}C NMR (100 MHz, DMSO- d_6), ppm: 102.1, 122.7, 127.6, 129.5, 130.6, 132.1, 132.5, 138.5, 143.2, 147.4, 151.9, 159.3, 167.7. MS: m/z 422 [$M + 1$]. Anal. Calcd. for $\text{C}_{15}\text{H}_5\text{F}_6\text{N}_3\text{O}_3\text{S}$: C, 42.77; H, 1.20; N, 9.97. Found: C, 42.74; H, 1.15; N, 10.03.

8-Nitro-6-(trifluoromethyl)-2-((4-(trifluoromethylphenyl)amino)-4H-benzo[e][1,3]thiazin-4-one (Vi). Yield: 90%. mp: 147–149°C. ^1H NMR (400 MHz, DMSO- d_6), ppm: 4.25 (s, 1H, –NH), 7.21 (d, 2H, $J = 8.8$ Hz, Ar–H), 7.82 (d, 2H, $J = 8.8$ Hz, Ar–H), 8.26 (s, 1H, Ar–H), 8.63 (s, 1H, Ar–H). ^{13}C NMR (100 MHz, DMSO- d_6), ppm: 116.5, 122.4, 124.1, 125.9, 126.5, 127.6, 129.2, 132.3, 132.6, 138.3, 142.7, 147.8, 159.3, 167.7. MS: m/z 436 [$M + 1$]. Anal. Calcd. for $\text{C}_{16}\text{H}_7\text{F}_6\text{N}_3\text{O}_3\text{S}$: C, 44.15; H, 1.62; N, 9.65. Found: C, 44.11; H, 1.60; N, 9.69.

Antitubercular assay. An evaluation was carried out on the antitubercular activity of the newly synthesized compounds (Va–Vi) against MDR-*Mtb* and *Mtb* H37Rv strains. Mycobacterial cultures, namely *Mtb* H37Rv (ATCC 27294) and MDR-*Mtb* (ATCC 35822), were obtained from the ATCC. For this investigation, a two-fold serial dilution from 125 to 0.1 μM was employed, as previously reported [39–43]. The MIC was the lowest dosage of the medication that inhibited bacterial growth. In a single experiment, the concentration of each molecule was measured in triplicate, and the mean \pm SD was calculated.

Cytotoxicity assay. A normal lung fibroblast cell line, known as WI-38, was used to test the cytotoxic effects of the synthesized compounds. The MTT assay was used to conduct the test. The cytotoxicity assay was carried out in accordance with our previously published work [44–46].

DprE1 inhibition studies. As per the reported literature [47], *Mtb* DprE1 was expressed and purified in *E. coli* cells. The Amplex Red/peroxidase-linked test was used to measure enzyme activity by the published protocol [48]. In summary, DprE1 (0.5 μ M) was incubated at 30°C in 20 mM glycylglycine pH 8.5, which also included 0.35 μ M horseradish peroxidase and 0.050 mM Amplex Red. 500 μ M FPR was added to start the reaction, and resorufin production was measured at 572 nm. A negative control was DMSO. The IC₅₀ value of the enzyme inhibitory activity was determined and contrasted with PBTZ169, a positive control.

Molecular docking. The docking investigation of potent compounds with the target protein was carried out using AutoDock Vina, which was expanded in UCSF Chimera. DprE1 (PDB ID: 4P8L), a receptor from the RCSB Protein Data Bank, was used in this instance. AutoDock Tools were used to prepare the DprE1 protein. Hydrogen atoms were initially added to the protein after water molecules were eliminated. The AutoDock Vina application is used to dock the ligands' structures with specific protein structures once the ligands' pdb and mol2 files are constructed using the ChemBioOffice tool. Using default values for the remaining parameters, the Lamarckian genetic algorithm calculating approach employs the ligand molecular coordinates from the original crystal structure as the center of the box. Only the optimal location with a root mean square deviation of less than one Å was chosen from all the docked outcomes. Utilizing UCSF Chimera and BIOVIA Discovery Studio Visualization, the ideal protein-ligand posture was illustrated. Additionally, utilizing the free web server <http://www.swissadme.ch/>, the drug-likeness of the compounds was assessed.

CONCLUSIONS

In conclusion, we report that new benzothiazinone derivatives (**Va–Vi**) were successfully synthesized under simple conditions using a multi-step methodology, and excellent yields of these novel compounds were achieved. Compounds (**Vf–Vi**) were shown to be potent when their antitubercular activity was evaluated against drug-sensitive *Mtb* H37Rv and MDR-TB strains. When SAR

was analyzed, it was shown that a modification in the nature of the substituent had a significant influence on antitubercular efficacy. With MIC values of 0.01 and 0.21 μ M for drug-resistant MDR-TB strains and drug-sensitive *Mtb* H37Rv strains, respectively, compound (**Vi**) was the most effective analogue. The DprE1 enzyme, a crucial enzyme for TB, is inhibited by compounds (**Vf**) and (**Vi**), according to the enzyme inhibition data. The IC₅₀ values of these compounds were similar to those of the reference drug PBTZ169, but they also had the advantage of being active against the MDR-TB strain. All of the newly synthesized compounds were shown to be non-cytotoxic, even at a concentration of 64 μ M, indicating that they have great promise as candidates for anti-infective drug development. According to molecular docking experiments, all of the potent compounds under investigation bind firmly to the target protein (PDB ID: 4P8L), which confirms excellent inhibitory efficacy against the DprE1 enzyme. This work introduces novel benzothiazinone compounds for further investigation in our search for new antitubercular agents with lower toxicity.

ACKNOWLEDGMENTS

The authors immensely express their indebted gratitude to the Management of BNM Institute of Technology for providing lab facilities to carry out this work. The authors extend their thanks and appreciation to Researchers supporting project (no. RSP-2024R160) King Saud University, Riyadh, Saudi Arabia.

FUNDING

This work was funded by the Korea Institute of Energy Technology Evaluation and Planning (KETEP) of the Republic of Korea (no. RS-2023-00255939). Byong-Hun Jeon thank Hanyang University, Seoul, Republic of Korea.

ETHICS APPROVAL AND CONSENT TO PARTICIPATE

This article does not contain any studies involving patients or animals as test objects.

Informed consent was not required for this article.

CONFLICT OF INTEREST

No conflicts of interest was declared by the authors.

AUTHOR CONTRIBUTION

The author MSR—investigation and writing of the article; the author AYJ—formal analysis, writing of the article; the author KYK—data curation and formal analysis; the author FA—software, visualization and validation; the author MKP—conceptualization, methodology, supervision, and proofreading; the author BHJ—guidance, supervision and proofreading.

DATA AVAILABILITY

The data that support the findings of this study are available from the corresponding author upon reasonable request.

SUPPLEMENTARY INFORMATION

The online version contains supplementary material available at <https://doi.org/10.1134/S1068162025010042>

REFERENCES

1. Fernandes, G.F.S., Thompson, A.M., Castagnolo, D., Denny, W.A., and Dos Santos, J.L., *J. Med. Chem.*, 2022, vol. 65, pp. 7489–7531.
<https://doi.org/10.1021/acs.jmedchem.2c00227>
2. Pflögr, V., Horvath, L., Stolarikova, J., Pal, A., Kordulakova, J., Bosze, S., Vinsova, J., and Kratky, M., *Eur. J. Med. Chem.*, 2021, vol. 223, pp. 113668.
<https://doi.org/10.1016/j.ejmech.2021.113668>
3. TB Reports.
<https://www.who.int/teams/global-tuberculosis-programme/tb-reports/global-tuberculosis-report>, 2023.
4. Raghu, M.S., Yogesh Kumar, K., Shamala, T., Alharti, F.A., Prashanth, M.K., and Jeon, B.H., *J. Biomol. Struct. Dyn.*, 2024, vol. 42, pp. 3307–3317.
<https://doi.org/10.1080/07391102.2023.2217928>
5. Bonde, C., Gawad, J., and Bonde, S., *Indian J. Tuberc.*, 2022, vol. 69, pp. 404–420.
<https://doi.org/10.1016/j.ijtb.2021.09.003>
6. Li, H. and Jogl, G., *Prot. Struct. Funct. Bioinform.*, 2013, vol. 81, pp. 538–543.
<https://doi.org/10.1002/prot.24220>
7. Wolucka, B.A., *FEBS J.*, 2008, vol. 275, pp. 2691–2711.
<https://doi.org/10.1111/j.1742-4658.2008.06395.x>
8. Lee, B.S. and Pethe, K., *Curr. Opin. Pharmacol.*, 2018, vol. 42, pp. 22–26.
<https://doi.org/10.1016/j.coph.2018.06.006>
9. Kolly, G.S., Boldrin, F., Sala, C., Dhar, N., Hartkoorn, R.C., Ventura, M., Serafini, A., Mckinney, J.D., Manganelli, R., and Cole, S.T., *Mol. Microbiol.*, 2014, vol. 92, pp. 194–211.
<https://doi.org/10.1111/mmi.12546>
10. Riccardi, G., Pasca, M.R., Chiarelli, L.R., Manina, G., Mattevi, A., and Binda, C., *Appl. Microbiol. Biotechnol.*, 2013, vol. 97, pp. 8841–8848.
<https://doi.org/10.1007/s00253-013-5218-x>
11. Prashanth, M.K., Revanasiddappa, H.D., Lokanatha Rai, K.M., and Veeresh, B., *Bioorg. Med. Chem. Lett.*, 2012, vol. 22, pp. 7065–7070.
<https://doi.org/10.1016/j.bmcl.2012.09.089>
12. Ramzan, F., Nabi, S.A., Lone, M.S., Imtiyaz, K., Urooj, L., Vishakha, V., Sharma, K., Rizvi, M.M.A., Shafi, S., Samim, M., Bano, S., and Javed, K., *ACS Omega*, 2023, vol. 8, pp. 6650–6662.
<https://doi.org/10.1021/acsomega.2c07153>
13. Makarov, V., Lechartier, B., Zhang, M., Neres, J., Sar, A.M., Raadsen, S.A., Hartkoorn, R.C., Ryabova, O.B., Vocat, A., Decosterd, L.A., Widmer, N., Buclin, T., Bitter, W., Andries, K., Pojer, F., Dyson, P.J., and Cole, S.T., *EMBO Mol. Med.*, 2014, vol. 6, pp. 372–383.
<https://doi.org/10.1002/emmm.201303575>
14. Wang, A., Ma, C., Chai, Y., Liu, X., Lv, K., Fu, L., Wang, B., Liu, M., Lu, L., *Eur. J. Med. Chem.*, 2020, vol. 200, p. 112409.
<https://doi.org/10.1016/j.ejmech.2020.112409>
15. Lv, K., You, X., Wang, B., Wei, Z., Chai, Y., Wang, B., Wang, A., Huang, G., Liu, M., and Lu, Y., *ACS Med. Chem. Lett.*, 2017, vol. 8, pp. 636–641.
<https://doi.org/10.1021/acsmchemlett.7b00106>
16. Lv, K., Tao, Z., Liu, Q., Yang, L., Wang, B., Wu, S., Wang, A., Huang, M., Liu, M., and Lu, Y., *Eur. J. Med. Chem.*, 2018, vol. 151, pp. 1–8.
<https://doi.org/10.1016/j.ejmech.2018.03.060>

17. Chikhale, R.V., Barmade, M.A., Murumkar, P.R., and Yadav, M.R., *J. Med. Chem.*, 2018, vol. 61, pp. 8563–8593.
<https://doi.org/10.1021/acs.jmedchem.8b00281>
18. Zhang, G., Howe, M., and Aldrich, C.C., *ACS Med. Chem. Lett.*, 2019, vol. 10, pp. 348–351.
<https://doi.org/10.1021/acsmchemlett.8b00634>
19. Gao, C., Peng, C., Shi, Y., You, X., Ran, K., Xiong, L., Ting-hong, Y., Zhang, L., Wang, N., Zhu, Y., Liu, K., Zuo, W., Yu, L., and Wei, Y., *Sci. Rep.*, 2016, vol. 6, p. 29717.
<https://doi.org/10.1038/srep29717>
20. Sivaiah, G., Raveesha, R., Benaka Prasad, S.B., Yogesh Kumar, K., Raghu, M.S., Alharti, F.A., Prashanth, M.K., and Jeon, B.H., *J. Mol. Struct.*, 2023, vol. 1275, p. 134728.
<https://doi.org/10.1016/j.molstruc.2022.134728>
21. Yousef, T.A., Alhamzani, A.G., Abou-Krishna, M.M., Kanthimathi, G., Raghu, M.S., Yogesh Kumar, K., Prashanth, M.K., and Jeon, B.H., *Heliyon*, 2023, vol. 9, p. e13460.
<https://doi.org/10.1016/j.heliyon.2023.e13460>
22. Sivaiah, G., Raveesha, R., Benaka Prasad, S.B., Kumar, K.Y., Raghu, M.S., Alharethy, F., Prashanth, M.K., and Jeon, B.H., *J. Mol. Struct.*, 2023, vol. 1289, p. 135877.
<https://doi.org/10.1016/j.molstruc.2023.135877>
23. Madaiah, M., Prashanth, M.K., Revanasiddappa, H.D., and Veeresh, B., *Arch. Pharm.*, 2014, vol. 347, pp. 370–380.
<https://doi.org/10.1002/ardp.201300289>
24. Madaiah, M., Prashanth, M.K., and Revanasiddappa, H.D., *Tetrahedron Lett.*, 2013, vol. 54, pp. 1424–1427.
<https://doi.org/10.1016/j.tetlet.2012.12.115>
25. Prashanth, M.K., Madaiah, M., Revanasiddappa, H.D., and Amruthesh, K.N., *ISRN Org. Chem.*, 2013, vol. 2013, pp. 1–12.
<https://doi.org/10.1155/2013/791591>
26. Kumar, C.B.P., Raghu, M.S., Prathibha, B.S., Prashanth, M.K., Kanthimathi, G., Kumar, K.Y., Parashuram, L., and Alharthi, F.A., *Bioorg. Med. Chem. Lett.*, 2021, vol. 44, p. 128118.
<https://doi.org/10.1016/j.bmcl.2021.128118>
27. Theodore, C.E., Sivaiah, G., Benaka Prasad, S.B., Kumar, K.Y., Raghu, M.S., Alharethy, F., Prashanth, M.K., and Jeon, B.H., *J. Mol. Struct.*, 2023, vol. 1294, p. 136341.
<https://doi.org/10.1016/j.molstruc.2023.136341>
28. Madaiah, M., Jayanna, B.K., Manu, A.S., Prashanth, M.K., Revanasiddappa, H.D., and Veeresh, B., *Arch. Pharm.*, 2017, vol. 350, p. e1600303.
<https://doi.org/10.1002/ardp.201600303>
29. Madaiah, M., Prashanth, M.K., Revanasiddappa, H.D., and Veeresh, B., *Med. Chem. Res.*, 2013, vol. 22, pp. 2633–2644.
<https://doi.org/10.1007/s00044-012-0265-x>
30. Prashanth, M.K. and Revanasiddappa, H.D., *Lett. Drug. Des. Discov.*, 2014, vol. 11, pp. 712–720.
<https://doi.org/10.2174/1570180811666131230235157>
31. Raghu, M.S., Yogesh Kumar, K., Veena, K., Pradeep Kumar, C.B., Almalki, A.S., Mani, G., Alasmay, F.A., and Prashanth, M.K., *J. Mol. Struct.*, 2022, vol. 1250, p. 131857.
<https://doi.org/10.1016/j.molstruc.2021.131857>
32. Raghu, M.S., Swarup, H.A., Prathibha, B.S., Yogesh Kumar, K., Pradeep Kumar, C.B., Alharti, F.A., Prashanth, M.K., and Jeon, B.H., *J. Mol. Struct.*, 2023, vol. 1285, p. 135502.
<https://doi.org/10.1016/j.molstruc.2023.135502>
33. Makarov, A.V., Cole, S.T., and Mollmann, U., *New Benzothiazinone Derivatives and Their Use as Anti-bacterial Agents*, Google Patents, 2011.
<https://patents.google.com/patent/WO2007134625A1/en>
34. Mikusova, K., Huang, H., Yagi, T., Holsters, M., Verecke, D., D’Haeze, W., Scherman, M.S., Brennan, P.J., McNeil, M.R., and Crick, D.C., *J. Bacteriol.*, 2005, vol. 187, pp. 8020–8025.
<https://doi.org/10.1128/jb.187.23.8020-8025.2005>
35. Amado, P.S.M., Woodley, C., Cristiano, M.L.S., and O’Neill, P.M., *ACS Omega*, 2022, vol. 7, pp. 40659–40681.
<https://doi.org/10.1021/acsomega.2c05307>

36. Lipinski, C.A., Lombardo, F., Dominy, D.W., and Feeney, P.J., *Adv. Drug Deliv. Rev.*, 2012, vol. 64, pp. 4–17. [https://doi.org/10.1016/s0169-409x\(00\)00129-0](https://doi.org/10.1016/s0169-409x(00)00129-0)
37. Veber, D.F., Johnson, S.R., Cheng, H.Y., Smith, B.R., Ward, K.W., and Kopple, K.D., *J. Med. Chem.*, 2022, vol. 45, pp. 2615–2623. <https://doi.org/10.1021/jm020017n>
38. Sebastian, S., Bernal, F.A., Wojtas, K.P., Keiff, F., Li, Y., Dahse, H.M., and Kloss, F., *J. Med. Chem.*, 2022, vol. 65, pp. 6748–6763. <https://doi.org/10.1021/acs.jmedchem.2c00098>
39. Pradeep Kumar, C.B., Raghu, M.S., Prathibha, B.S., Prashanth, M.K., Yogesh Kumar, K., Revanasiddappa, H.D., Jayanna, B.K., and Alharthi, F.A., *Bioorg. Med. Chem. Lett.*, 2021, vol. 36, p. 127810. <https://doi.org/10.1016/j.bmcl.2021.127810>
40. Raghu, M.S., Pradeep Kumar, C.B., Prasad, K.N.N., Chandrasekhar, S., Yogesh Kumar, K., Prashanth, M.K., and Veeresh, B., *ACS Comb. Sci.*, 2020, vol. 22, p. 509–518. <https://doi.org/10.1021/acscombsci.0c00038>
41. Madaiah, M., Prashanth, M.K., Revanasiddappa, H.D., and Veeresh, B., *New J. Chem.*, 2016, vol. 40, pp. 9194–9204. <https://doi.org/10.1039/C6NJ02069K>
42. Raghu, M.S., Pradeep Kumar, C.B., Yogesh Kumar, K., Prashanth, M.K., Alshahrani, M.Y., Ahmad, I., and Jain, R., *Bioorg. Med. Chem. Lett.*, 2022, vol. 60, p. 128604. <https://doi.org/10.1016/j.bmcl.2022.128604>
43. Veena, K., Raghu, M.S., Kumar, K.Y., Kumar, C.B.P., Alharti, F.A., Prashanth, M.K., and Jeon, B.H., *J. Mol. Struct.*, 2022, vol. 1269, p. 133822. <https://doi.org/10.1016/j.molstruc.2022.133822>
44. Sivaiah, G., Raghu, M.S., Benaka Prasad, S.B., Anusuya, A.M., Yogesh Kumar, K., Alharethy, F., Prashanth, M.K., and Jeon, B.H., *J. Mol. Struct.*, 2024, vol. 1309, p. 138223. <https://doi.org/10.1016/j.molstruc.2024.138223>
45. Veena, K., Raghu, M.S., Kumar, K.Y., Dahlous, K.A., Bahajjaj, A.A.A., Mani, G., Jeon, B.H., and Prashanth, M.K., *J. Mol. Struct.*, 2022, vol. 1258, p. 132674. <https://doi.org/10.1016/j.molstruc.2022.132674>
46. Theodore, C.E., Anusuya, A.M., Sivaiah, G., Jain, R., Ananda Kumar, C.S., Benaka Prasad, S.B., Raghu, M.S., Alharti, F.A., Prashanth, M.K., and Jeon, B.H., *J. Mol. Struct.*, 2023, vol. 1288, p. 135765. <https://doi.org/10.1016/j.molstruc.2023.135765>
47. Neres, J., Pojer, F., Molteni, E., Chiarelli, L.R., Dhar, N., Boy-Röttger, S., Buroni, S., Fullam, E., Degiacomi, G., Lucarelli, A.P., Read, R.J., Zanoni, G., Edmondson, D.E., De Rossi, E., Pasca, M.R., McKinney, J.D., Dyson, P.J., Riccardi, G., Mattevi, A., Cole, S.T., and Binda, C., *Sci. Transl. Med.*, 2012, vol. 4, p. 150ra121. <https://doi.org/10.1126/scitranslmed.3004395>
48. Neres, J., Hartkoorn, R.C., Chiarelli, L.R., Gadupudi, R., Pasca, M.R., Mori, G., Farina, D., Savina, S., Makarov, V., Kolly, G.S., Molteni, E., Binda, C., Dhar, N., Ferrari, S., Brodin, P., Delorme, V., Landry, V., Ribeiro, A.L., Venturilli, A., Saxena, P., Pojer, F., Carta, A., Luciani, R., Porta, A., Zanoni, G., De Rossi, E., Costi, M.P., Riccardi, G., and Cole, S.T., *ACS Chem. Biol.*, 2015, vol. 10, pp. 705–714. <https://doi.org/10.1021/cb5007163>

Publisher's Note. Pleiades Publishing remains neutral with regard to jurisdictional claims in published maps and institutional affiliations. AI tools may have been used in the translation or editing of this article.